PERGAMON

Chemosphere 42 (2001) 655–661

CHEMOSPHERE

Excimer laser fragmentation-fluorescence spectroscopy as a method for monitoring ammonium nitrate and ammonium sulfate particles

Christopher J. Damm [a], Donald Lucas [b,*], Robert F. Sawyer [a,1], Catherine P. Koshland [c]

[a] *Department of Mechanical Engineering, University of California, Berkeley, CA 94720, USA*
[b] *Environmental Energy Technologies Division, Lawrence Berkeley National Laboratory, MS 70-108B, Berkeley, CA 94720, USA*
[c] *School of Public Health, 751 University Hall, University of California, Berkeley, CA 94720, USA*

Abstract

Excimer laser fragmentation-fluorescence spectroscopy (ELFFS) is shown to be an effective detection strategy for ammonium nitrate and ammonium sulfate particles at atmospheric pressure and room temperature. Following photofragmentation of the ammonium salt particle, fluorescence of the NH fragment is observed at 336 nm. The fluorescence signal is shown to depend linearly on particle surface area for laser intensities varying from 1.2×10^8 to 6×10^8 W/cm^2. The 100 shot (1 s) detection limits for ammonium nitrate range from 20 ppb for 0.2 μm particles to 125 ppb for 0.8 μm particles, where these concentrations are expressed as moles of ammonium ion per mole of air. For ammonium sulfate, the 100 shot (1 s) detection limits vary from 60 ppb for 0.2 μm particles to 500 ppb for 1 μm particles. These detection limits are low enough to measure ammonium salt particles that form in the exhaust of combustion processes utilizing ammonia injection as a nitric oxide control strategy.

Keywords: Aerosol measurement; Air pollution; Combustion; Diagnostics

1. Introduction

Ammonium nitrate and ammonium sulfate are of concern as major air pollutants. Ammonium nitrate is found in areas where there are high NO_x and high ammonia emissions, while ammonium sulfate is prevalent where both ammonia and SO_2 are abundant. In California, they contribute approximately 25% to the total PM_{10} mass on an annual average basis. Their contribution to total $PM_{2.5}$ particles is even greater (~45%) (Chow et al., 1992). These accumulation mode particles have been shown to pose a threat to human health due to their ability to penetrate deep into the lung and deposit. Their size also makes them efficient light scatterers, so their presence can lead to visibility impairment and can affect the global energy balance. Accumulation mode particles are able to migrate over great distances so that their effects are not limited to the region where they are first formed. Ammonium nitrate and sulfate also impact the acidity of atmospheric aerosols.

Ammonium nitrate and ammonium sulfate concentrations are usually measured by collecting particulate matter on a filter. As the ammonium salt exists in equilibrium with the corresponding gaseous acid (nitric or sulfuric acid) and ammonia, the filter may lose mass

* Corresponding author. Tel.: +1-510 486 7002; fax: +1-510 486 7303.
E-mail address: d_lucas@lbl.gov (D. Lucas).
[1] 72 Hesse Hall, University of California, Berkeley, CA 94720, USA.

0045-6535/01/$ - see front matter
PII: S0045-6535(00)00239-3

due to particle-to-gas conversion, making accurate measurements of ammonium salt particle concentrations difficult. Filter collection techniques also yield only time integrated concentrations, with collection times ranging from hours to days.

Real-time measurement of ammonium nitrate particles would be useful in understanding and modeling aerosol formation in combustion exhausts and in the atmosphere. Real-time characterization of ammonium sulfate particles has been performed using laser desorption/ionization mass spectroscopy (McKeown et al., 1991; Mansoori et al., 1994) to study ammonium sulfate particles (McKeown et al., 1991). Aerosol time-of-flight mass spectroscopy (ATOFMS) has been used to perform real-time chemical component analysis on individual atmospheric aerosol particles, including ammonium nitrate and ammonium sulfate (Noble and Prather, 1996).

The goal of this investigation is to determine whether excimer laser fragmentation-fluorescence spectroscopy (ELFFS) can be used to make quantitative measurements of ammonium nitrate and ammonium sulfate particles.

1.1. Excimer laser fragmentation-fluorescence spectroscopy

Many molecules of environmental interest have only weakly or non-fluorescing excited electronic states, due to a large degree of internal energy transfer and/or long excited state lifetimes. ELFFS employs photofragmentation of larger molecules to form less complex, fluorescent signature species, from which the presence of the parent can be detected. For example, NH is a signature fragment for amines and C–Cl is a signature species for chlorinated hydrocarbons. Using a single laser, the signature species may be excited by excess energy following photofragmentation of the parent molecule. In this case, fluorescence may be observed during and immediately after the photofragmentation laser pulse.

Our laboratory has used ELFFS to detect gaseous ammonia (Buckley et al., 1998), toxic metals such as Pb, Cr and Ni (Buckley, 1995; Buckley et al., 1996a,b) and chlorinated hydrocarbons (McEnally et al., 1994a,b) in post-flame gases at atmospheric pressure. Recently, the technique has been employed to detect alkali species in pressurized boilers (Hartinger et al., 1993, 1994). Many other species have been detected in laboratory studies at low pressure, but have not been attempted in realistic atmospheric pressure monitoring environments; the reader is referred to a recent review (Simeonsson and Sausa, 1996) for details.

2. Methods

A schematic of the apparatus is depicted in Fig. 1. The experiments are conducted 0.5 cm above a 3 cm diameter vertical tube issuing into quiescent room air. Ammonium nitrate and ammonium sulfate salt solu-

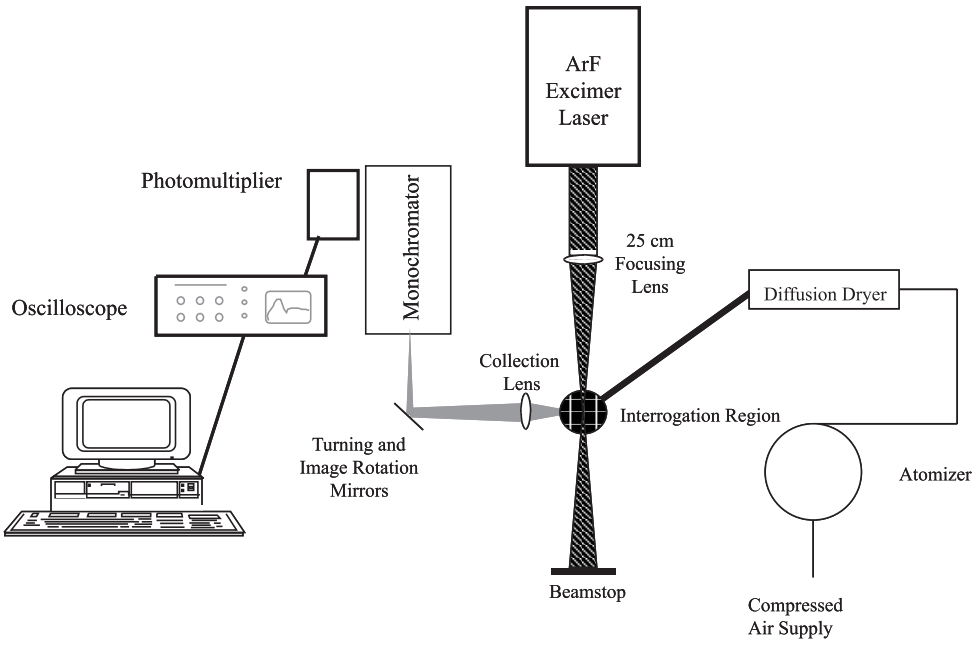

Fig. 1. Experimental apparatus.

tions of various molarities are atomized to form nominal 2 μm droplets by a TSI Model 9302A atomizer. As water evaporates from the droplet, the salt precipitates to form a solid ammonium nitrate or ammonium sulfate particle. As long as the relative humidity is below the deliquescence relative humidity (62% for ammonium nitrate, 80% for ammonium sulfate at 298 K) (Seinfeld and Pandis, 1998), no aqueous phase ammonium nitrate/sulfate remains. The particles pass through a diffusion dryer to ensure that the relative humidity is sufficiently low (measured to be 45%). Flows are metered by rotometers.

An ArF excimer laser (Lambda Physik EMG 102 MSC) develops 120 mJ pulses of 193 nm light, which are focused into the interrogation region using a 25 cm focal length UV-grade fused-silica lens. This creates a detection region with a minimum cross-section of 2 by 0.5 mm. When a lower laser intensity is desired, the beam is sent through an array of screens before it reaches the interrogation region. The peak intensity at the focal region of 6×10^8 W/cm^2 is sufficient to cause ionization of an ammonium nitrate or ammonium sulfate molecule (Thomson et al., 1997). The laser pulse energy is measured using a Gentech ED-500 joulemeter.

The detection region is imaged onto the entrance slit of a 0.3 m McPherson scanning monochromator with a single plano-convex lens. The measurements are made using a 7.5 cm focal length, 2.5 cm diameter fused silica lens positioned roughly 9 cm from the detection region to focus the detection region through the monochromator slit. All spectra presented here were collected with a horizontal slitwidth of 0.4 mm, which corresponds to a bandpass of 1.1 nm. A 280 nm cut-on high-pass glass filter (Schott WG-280, CVI Laser) mounted at the entrance slit of the monochromator helps reject scattered 193 nm light.

The light passed by the monochromator enters a Hamamatsu R928 photomultiplier tube, the signal generated is digitized by a LeCroy 9410 digital oscilloscope and sent to an IBM-compatible PC for storage and processing. ELFFS spectra are obtained coincident with the laser pulse (pulse width = 20 ns). NH fluorescence from the photofragmented ammonium nitrate/sulfate molecules is observed at 336 nm. There is interference in the photofragmentation spectrum of both room air and typical combustion exhaust from N_2 (C–B) fluorescence at 337.1 nm. This is not problematic because the N_2 concentration is constant in these environments and thus the N_2 contribution to the signal can be subtracted from the measured signal.

3. Results and discussion

Fig. 2 shows single-shot fluorescence spectra from the photofragmentation of ammonium nitrate and ammonium sulfate particles, as well as the background spectrum. These spectra were obtained by atomizing and drying a 0.4 M solution of ammonium nitrate and a 0.2 M solution of ammonium sulfate; the ammonium ion concentrations are thus the same for the two solutions. The laser was fired at 2 Hz while the monochromator was scanned at a rate of 5 nm/min. The peaks for the ammonium salt particles are centered at 336 nm and are attributed to NH(A–X) emission. Based on the observed full width at half maximum (FWHM) of roughly 2 nm, compared with the monochromator bandpass of 1.1 nm, it is likely that these peaks are a combination of the (0–0) and (1–1) emission bands, the former at 336.0 nm and the latter at 337.0 nm (Pearse and Gaydon, 1963). The only feature apparent in the room air spectrum is the aforementioned N_2(C–B) emission at 337.1 nm, which is the prominent line in the nitrogen laser. The fluorescence was subsequently monitored at 336.0 nm, where the monochromator is able to reject most, but not all of the N_2 emission. The spectra are plotted as a Savitsky–Golay rolling average of five points to reduce the noise.

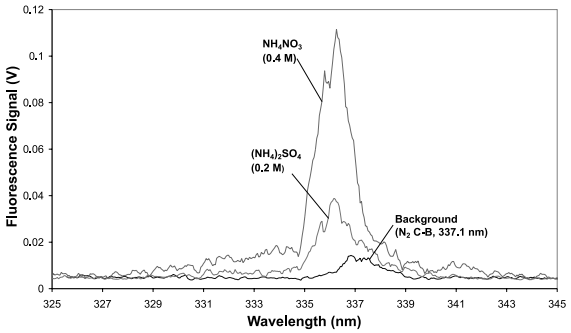

Fig. 2. NH fluorescence from ammonium nitrate and sulfate particles.

The fluorescence signal was measured while varying the droplet solution molarity with the results summarized in Tables 1 and 2. The reported signal is an average of 1000 laser shots and is uncertain by ±10% (1 S.D.). The particle diameter was calculated assuming that the atomizer generates monodisperse 2 μm droplets and the droplets dry to form spherical ammonium salt particles. The validity of this assumption is addressed later when the actual particle size distribution is presented. Figs. 3 and 4 show how the fluorescence signal varies with the ammonium ion concentration of the flow through the interrogation region for ammonium nitrate and ammonium sulfate. Three different laser pulse energies were used. The signal levels off as the ammonium ion concentration increases. The plots do not go through the origin because with a 1.1 nm bandwidth it is not possible to reject all of the 337.1 nm N_2 band when monitoring at 336.0 nm. This behavior contrasts with the results for gaseous ammonia in N_2, in which the signal was linear

Table 1
Ammonium nitrate measurements

Solution molarity	NH_4 Conc. (ppm)	Particle diameter (μm)	Particle S.A. (sq. μm)	Fluorescence signal (mV)
Background				12.0
0.02	0.1	0.20	0.12	20.0
0.06	0.3	0.28	0.25	26.4
0.1	0.5	0.34	0.35	34.3
0.2	1.0	0.42	0.56	47.4
0.3	1.5	0.48	0.73	49.9
0.4	2.0	0.53	0.89	58.8
0.5	2.5	0.57	1.03	71.9
0.6	3.0	0.61	1.17	74.2
0.8	4.0	0.67	1.41	88.9
1.6	8.0	0.84	2.24	120.8

Table 2
Ammonium sulfate measurements

Solution molarity	NH_4 Conc. (ppm)	Particle diameter (μm)	Particle S.A. (sq. μm)	Fluorescence signal (mV)
Background				6.9
0.02	0.1	0.23	0.16	9.9
0.06	0.3	0.33	0.34	11.0
0.1	0.5	0.39	0.48	13.5
0.2	1.0	0.49	0.76	14.4
0.3	1.5	0.56	1.00	17.5
0.4	2.0	0.62	1.21	19.2
0.5	2.5	0.67	1.40	20.0
0.6	3.0	0.71	1.59	23.4
0.8	4.0	0.78	1.92	26.4
1.6	8.0	0.99	3.05	33.9

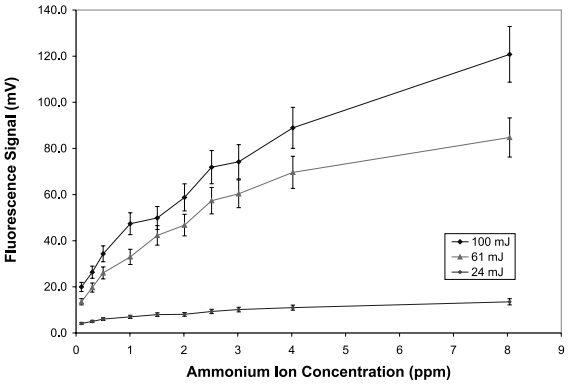

Fig. 3. NH fluorescence from ammonium nitrate particles in air for different laser pulse energies. The non-zero intercepts are due to N_2 (C–B) emission at 337.1 nm. The concentration is expressed as moles of ammonium ion per mole of air in the interrogation volume.

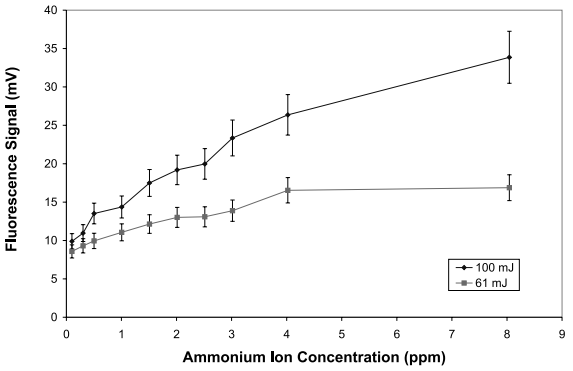

Fig. 4. NH fluorescence from ammonium sulfate particles in air for different laser pulse energies.

with NH_3 concentration up to 120 ppm, as depicted in Fig. 5. As the particle diameter increases with the concentration, the non-linearity of the signal depicted in Figs. 3 and 4 is likely due to the decrease in the surface area to volume ratio of the particles in the interrogation region. This suggests that the laser intensity is not sufficient to fully vaporize the particles, and the pulse is ablating molecules from the surface of the particle. As the particle size increases, the surface area-to-volume ratio gets smaller. In effect, a larger percentage of ammonium ions are on the inside of the particle where they are not available to take part in the photofragmentation-fluorescence process.

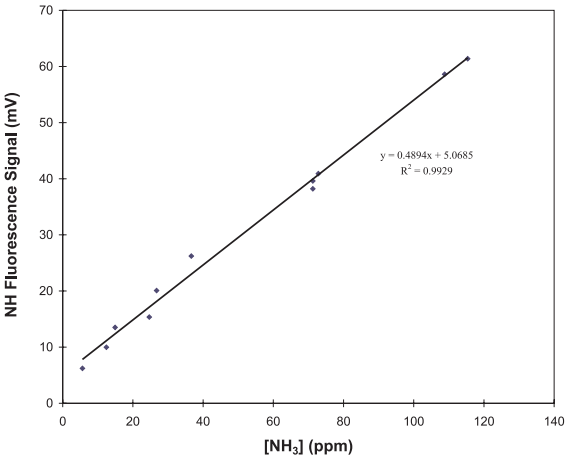

Fig. 5. NH fluorescence from ammonia gas.

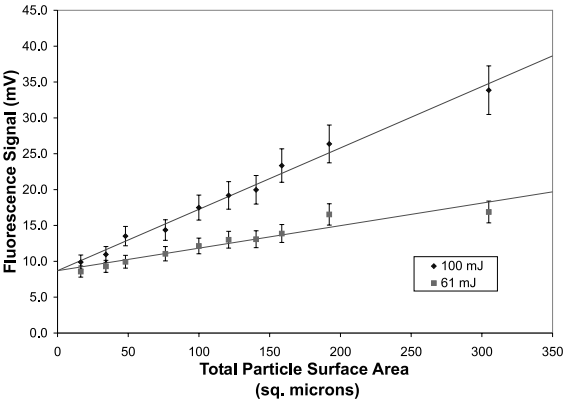

Fig. 7. NH fluorescence versus total particle surface area in the interrogation volume for ammonium sulfate.

Plots of the fluorescence signal versus particle surface area, shown in Figs. 6 and 7, confirm that the particles are not being fully vaporized. There is a linear relationship between the fluorescence signal and the total particle surface area in the interrogation volume. This suggests that only the molecules on the surface of the particles are participating in the photofragmentation-fluorescence.

To simplify the analysis presented in Figs. 6 and 7, the total surface area in the interrogation volume is calculated by assuming that the particles were monodisperse for each of the different solution concentrations. To test this assumption, the particle size distribution was measured with a TSI 3071A scanning mobility particle sizer (SMPS) and counter (CPC 3025A) for several different molarities of ammonium nitrate solution. As expected, the distributions are not monodisperse, as shown in Fig. 8. The geometric standard deviation (GSD) is approximately 2. (The GSD for a monodisperse aerosol is 1.) However, the median diameter is close to the calculated nominal diameter, and more importantly, the measured total particle surface area per volume correlates well with the value for surface area calculated assuming a monodisperse aerosol (Fig. 9). Therefore, the conclusion that the fluorescence signal varies linearly with total particle surface area remains valid. The particle size range that the SMPS is able to measure precluded us from determining the particle size distribution for all of the solution concentrations used. Thus, the calculated surface area rather than a measured surface area is used in Figs. 6 and 7.

It is important to address whether the observed fluorescence is from the desorption/ionization photofragmentation of the ammonium nitrate/sulfate or from the ammonia gas which exists along with nitric acid/sulfuric acid in equilibrium with the ammonium nitrate/sulfate.

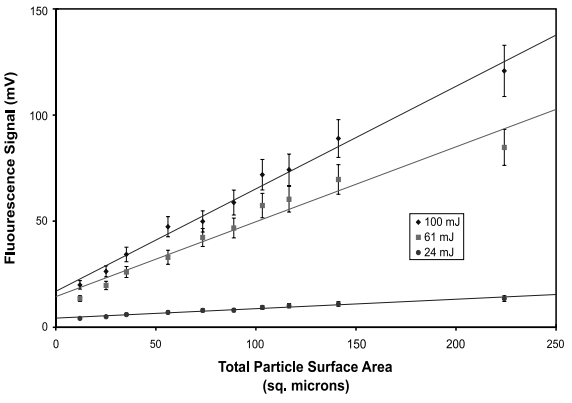

Fig. 6. NH fluorescence versus total particle surface area in the interrogation volume for ammonium nitrate.

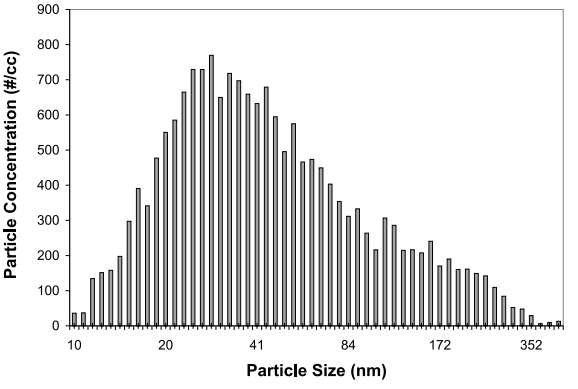

Fig. 8. Particle size distribution of atomized and dried ammonium nitrate solution (2×10^{-4} M). The median diameter is 39 nm. The GSD is 2.2.

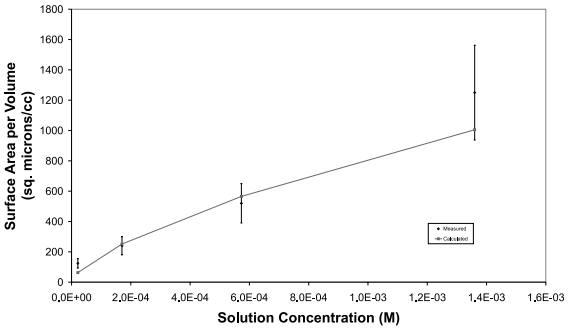

Fig. 9. Calculated and measured (w/scanning mobility particle sizer) surface area densities in the interrogation region for ammonium nitrate.

Assuming an equilibrium between the particles, ammonia gas and gaseous nitric acid, equilibrium calculations show that at a temperature of 295 K, the concentration of ammonia gas is 4 ppb, which yields a fluorescence signal of 0.25 mV, negligible compared to the measured signal.

The S.D. of the background spectrum is 5.6 mV. Defining the minimum detectable peak as 3 times the standard deviation of the background, the single-shot detection limit for ammonium nitrate in air at room temperature ranges from 0.2 ppm for the 0.2 μm particles to 1 ppm for the 0.8 μm particles (Table 3). For ammonium sulfate, the single shot detection limit varies from 0.6 ppm for 0.2 μm particles to 5 ppm for 1 μm particles. If the majority of noise in the spectrum is white noise, then it will follow Poisson's statistics, and averaged signals will be reduced in noise by a factor of $\sqrt{N}$, where N is the number of averaged laser shots. Averaging 100-shots, which is possible in 1 s of measurement time using commercially available excimer lasers, would decrease the detection limits by a factor of 10. The detection limits could be significantly improved if a 336 nm filter were used instead of the monochromator. Note that the detection limits would be 4–8 times higher (worse) in post-combustion gases due to the presence of water vapor, which has a large NH quenching cross-section relative to nitrogen and oxygen (Buckley et al., 1998).

4. Conclusion

ELFFS is shown to be a promising technique for real-time monitoring of ammonium nitrate and ammonium sulfate particles. For the laser intensities used, the fluorescence signal is dependent on particle size. Therefore, in order to obtain quantitative measurements of ammonium nitrate concentration, it is necessary to either use a sufficient laser intensity so that all of the solid is vaporized or make measurements to characterize the particle size distribution.

The single shot detection limits achieved are on the order of 1 ppm. These are low enough for measuring ammonium salt particle concentrations in the exhaust of combustion devices that utilize ammonia injection to reduce nitric oxide emissions. Any unreacted gas phase ammonia would have to be separated with a denuder before the measurement to avoid interference from the photofragmentation-fluorescence of ammonia. The detection limits are not low enough for ambient measurements of ammonium nitrate concentration, where a detection limit of approximately 1 ppb (which corresponds to a mass concentration of 3 $\mu g/m^3$ for ammonium nitrate and 5 $\mu g/m^3$ for ammonium sulfate) is required. This limit may be attainable if the monochromator were replaced with a 336 nm filter.

Acknowledgements

This work was funded by the US National Institute for Environmental Health Sciences, NIH grant P42-ES04705.

Table 3
Detection limits

Ammonium nitrate		Ammonium sulfate	
Particle diameter (μm)	100-Shot detection limit (ppb)	Particle diameter (μm)	100-Shot detection limit (ppb)
0.20	21	0.23	56
0.28	35	0.33	124
0.34	38	0.39	128
0.42	48	0.49	226
0.48	67	0.56	240
0.53	73	0.62	275
0.57	71	0.67	324
0.61	82	0.71	309
0.67	88	0.78	348
0.84	125	0.99	503

References

Buckley, S.G., 1995. Detection of toxic metals in combustion systems, Mechanical Engineering. University of California Press, Berkeley, CA.

Buckley, S.G., Damm, C.J., Vitovec, W.M., Sgro, L.A., Sawyer, R.F., Koshland, C.P., Lucas, D., 1998. Ammonia detection and monitoring with photofragmentation-fluorescence. Appl. Opt. 37 (36), 8382–8391.

Buckley, S.G., Koshland, C.P., Sawyer, R.F., Lucas, D., 1996a. A real-time monitor for toxic metals emissions from combustion systems. Proc. Combust. Inst., Vol. 26.

Buckley, S.G., McEnally, C.S., Sawyer, R.F., Koshland, C.P., Lucas, D., 1996b. Metal emissions monitoring using excimer laser fragmentation fluorescence spectroscopy. Combust. Sci. Technol. 118 (1–3), 169–188.

Chow, J.C., Watson, J.G., Lowenthal, D.H., Soloman, P.A., Magliano, K.L., Ziman, S.D., Richards, L.W., 1992. PM_{10} source apportionment in California's San-Joaquin valley. Atmos. Environ. 26A (18), 3335–3354.

Hartinger, K.T., Monkhouse, P.B., Wolfrum, J., 1993. Determination of alkali traces in coal combustion by excimer laser induced fragmentation fluorescence. Ber. Bunsenges. Phys. Chem. 97 (12), 1731–1734.

Hartinger, K.T., Monkhouse, P.B., Wolfrum, J., Baumann, H., Bonn, B., 1994. Determination of flue gas alkali concentrations in fluidized-bed coal combustion by excimer-laser-induced fragmentation fluorescence. Proc. Combust. Inst., Vol. 25.

Mansoori, B., Johnston, M., Wexler, A., 1994. Quantitation of ionic species in single microdroplets by on-line laser desorption/ionization. Anal. Chem. 66 (21), 3681–3687.

McEnally, C.S., Sawyer, R.F., Koshland, C.P., Lucas, D., 1994a. In situ detection of hazardous waste. Proc. Combust. Inst., Vol. 25.

McEnally, C.S., Sawyer, R.F., Koshland, C.P., Lucas, D., 1994b. Sensitive in situ detection of chlorinated hydrocarbons in gas mixtures. Appl. Opt. 33 (18), 3977–3984.

McKeown, P., Johnston, M., Murphy, D., 1991. On-line single-particle analysis by laser desorption mass spectrometry. Anal. Chem. 63 (18), 2069–2073.

Noble, C., Prather, K.J., 1996. Real-time measurement of correlated size and composition profiles of individual atmospheric aerosol particles. Eviron. Sci. Technol. 30 (9).

Pearse, R.W.B., Gaydon, A.G., 1963. The identification of Molecular Spectra, third ed. Wiley, New York.

Seinfeld, J.H., Pandis, S.N., 1998. Atmospheric Chemistry and Physics. Wiley, New York.

Simeonsson, J.B., Sausa, R.C., 1996. A critical review of laser photofragmentation fragment detection techniques for gas phase chemical analysis. Appl. Spectro. Rev. 31 (1–2), 1–72.

Thomson, D.S., Middlebrook, A.M., Murphy, D.M., 1997. Threshold for laser-induced ion formation from aerosols in a vacuum using ultraviolet and vacuum-ultraviolet laser wavelengths. Aerosol Sci. Technol. 26 (6), 544–559.